

Interpretable Company Similarity with Sparse Autoencoders

Marco Molinari^{*,1} and Victor Shao^{*,1} and Vladimir Tregubiak^{*,1}
Abhimanyu Pandey¹ and Mateusz Mikolajczak¹ and Sebastião Kuznetsov Ryder Torres Pereira¹

¹ LSE.AI, London School of Economics and Political Science
<https://lseai.org>

Correspondence: m.molinari1@lse.ac.uk

^{*}Equal Contribution

Abstract

Determining company similarity is a vital task in finance, underpinning hedging, risk management, portfolio diversification, and more. Practitioners often rely on sector and industry classifications to gauge similarity, such as SIC-codes and GICS-codes – the former being used by the U.S. Securities and Exchange Commission (SEC), and the latter widely used by the investment community. Since these classifications can lack granularity and often need to be updated, using clusters of embeddings of company descriptions has been proposed as a potential alternative, but the lack of interpretability in token embeddings poses a significant barrier to adoption in high-stakes contexts. Sparse Autoencoders (SAEs) have shown promise in enhancing the interpretability of Large Language Models (LLMs) by decomposing LLM activations into interpretable features. We apply SAEs to company descriptions, obtaining meaningful clusters of equities in the process. We benchmark SAE features against SIC-codes, Industry codes, and Embeddings. Our results demonstrate that SAE features not only replicate but often surpass sector classifications and embeddings in capturing fundamental company characteristics. This is evidenced by their superior performance in correlating monthly returns – a proxy for similarity – and generating higher Sharpe ratio co-integration strategies, which underscores deeper fundamental similarities among companies.

1 Introduction

Accurately assessing the similarity of companies is an integral task in finance, key to risk management and portfolio diversification (Delphini et al., 2019; Katselas et al., 2017). Hedging, a practice that relies on converse investments in related assets, is a prominent example of a financial strategy that requires a detailed understanding of the similarity between two companies.

Traditional modes of company comparisons rely on relative returns and discrete classifications, e.g. SIC codes or the Global Industry Classification System (GICS), which categorizes companies into 11 sectors and 163 sub-industries (MSCI, 2020). Relying on return spreads can be effective but is not foolproof, as market volatility, economic shifts, business fundamental changes, and temporal factors can disrupt them (Loretan and English, 2000).

Additionally, systems like GICS are limited, as the restricted granularity of a discrete classification system limits dynamic interpretations of companies' operations, as it falls short in accounting for the duality of certain companies, particularly in emerging industries (Winton, 2018).

This is particularly important for pairs trading, a market-neutral strategy based on mean-reverting return spreads (Ehrman, 2012). Employing a pairs trading strategy with fundamentally similar companies whose returns are co-integrated could lessen the risk of deviation from historical trends (Raghava and Bharadwaj, 2014).

Clustering embeddings of company descriptions has been proposed as a measure of similarity (Vamvourellis et al., 2023), but token embeddings are not interpretable, and this uncertainty is undesirable in the financial sector.

SAEs have the potential to provide an efficient measure of company similarity by decomposing large amounts of financial data into interpretable features (Chen et al., 2020). Moreover, SAEs have recently been applied to LLMs resulting in interpretable decompositions of neural activations (Huben et al., 2024). This motivates their application to textual company descriptions. We are the first, to the best of our knowledge, to compute company similarity using SAEs and SEC filings.

1.1 Sparse AutoEncoders

The linear representation hypothesis posits that LLMs linearly represent concepts in neuron acti-

vations (Park et al., 2024). However, neuron activations are notoriously superpositioned (Elhage et al., 2022), SAEs enhance the interpretability of LLMs by writing neuron activations as a linear combination of sparse features (Bricken et al., 2023). This reduces the superposition and restores the interpretability (Huben et al., 2024). SAEs have recently been applied both in mechanistic interpretability (Nanda et al., 2023; Conmy et al., 2023; Marks et al., 2024) of LLMs, and in deep learning more broadly (Chen and Guo, 2023). SAEs have been scaled to medium size and large Language Models (LMs), such as GPT4 (Templeton et al., 2024; Gao et al., 2024).

The Sparse Autoencoder (SAE) learns a reconstruction $\hat{\mathbf{x}}$ as a sparse linear combination of features $\mathbf{y}_i \in \mathbb{R}^{d_s}$ for a given input activation $\mathbf{x} \in \mathbb{R}^{d_m}$ with d_m as the Large Language Model (LLM)’s hidden size and:

$$d_s = k d_m, \quad \text{with } k \in \{2^n \mid n \in \mathbb{N}_+\}. \quad (1)$$

The decoder element of the SAE is given as:

$$(\hat{\mathbf{x}} \circ \mathbf{f})(\mathbf{x}) = \mathbf{b}_d + \mathbf{W}_d \mathbf{f}(\mathbf{x}) \quad (2)$$

where $\mathbf{b}_d \in \mathbb{R}^{d_m}$ is the bias term of the decoder, and \mathbf{W}_d is the decoder matrix with columns $\mathbf{v}_i \in \mathbb{R}^{d_m}$, and $\mathbf{f}(\mathbf{x})$ denotes the feature activations, which are described by:

$$\mathbf{f}(\mathbf{x}) = \text{TopK}(\mathbf{W}_e(\mathbf{x} - \mathbf{b}_d) + \mathbf{b}_e) \quad (3)$$

where $\mathbf{b}_e \in \mathbb{R}^{d_s}$ is the bias term of the encoder, and \mathbf{W}_e is the encoder matrix with columns $\mathbf{w}_i \in \mathbb{R}^{d_s}$. The loss function, which also corresponds to the output’s mean-squared error (MSE) is defined by:

$$\mathcal{L} = \|\mathbf{x} - \hat{\mathbf{x}}_2\|^2 \quad (4)$$

The choice of a TopK function rather than ReLU or L1 Regularization autoencoders is due to TopK having been empirically shown to outperform the latter in balancing sparsity and reconstruction accuracy (Gao et al., 2024).

1.2 Our contributions

- We apply an open source SAE (EleutherAI, 2024) to Llama 3 8B (Dubey et al., 2024), and extract interpretable features from SEC filings.
- We release a dataset containing company descriptions, extracted features, and returns, to support further research.

- We train a Siamese Network to obtain expected correlations from company descriptions, and construct a minimum spanning tree of stocks where correlated stocks are connected. We then perform hierarchical clustering with results comparable to, or better, than Embeddings, SIC-codes, and Industry categorizations.
- We demonstrate that a combined model, integrating SAE features with SIC-codes and Industry categorizations, significantly outperforms standalone approaches in explaining pairwise correlations, showing that our method can enhance industry classifications.
- We validate the applicability of our features via co-integration pairs trading strategies, and show that a strategy based on sparse features leads to a higher Sharpe ratio, demonstrating the potential for wider uses within finance.

2 Methodology

2.1 Dataset

Publicly listed companies in the U.S. submit annual financial performance reports to the Securities and Exchange Commission (SEC) which include information on a company’s operations, such as product specifics, subsidiaries, competition, and other financial details (SEC, 2023). We consider 220,275 annual reports from 1993 to 2020, ignoring any delists, accompanied by related meta-data on Company Name, Year, SIC-code, and CIK number (a unique SEC corporation identifier). CIK numbers are mapped to their corresponding publicly traded ticker symbol, from which the monthly logged returns are retrieved via Yahoo Finance (2024). Due to a lack of publicly available mappings between CIK codes and GICS classifications, we utilize: (1) SIC-codes, and (2) the industry/major-division categorization¹ (U.S. Occupational Safety and Health Administration, 2001). We remove entries with missing or very short: company descriptions, ticker information, or monthly returns. Next, company descriptions are tokenized using Meta’s Llama 3 8B Tokenizer (Dubey et al., 2024). We further refine the dataset by retaining only annual reports that have token counts within the context window, and are consistently available for at least five years,

¹The first 3 digits of the SIC code splits companies into 12 industry/major-divisions, referred to hereafter as BISC (Broader Industry Sector Code).

leaving us with a dataset of 27,722 reports. In our analysis, we ignore pre-1996 as the sample size is too small.

We employ forward testing in our experiments: when any training is done on year t , we report and use the predicted results on $t + 1$. Our dataset analysis finds that only 0.24% of subsequent company descriptions are identical, with 0.54% within a normalized Levenshtein distance of 0.01, and 12.34% within 0.05. Forward-testing is more robust than out-of-sample testing (Pardo, 1992), and since the descriptions are not repeated across years, the model remains generalized.

2.2 Feature summing

In this work, we face the challenge of comparing sparse feature sequences of arbitrary lengths, where best practices are not well-established, though max-pooling has been proposed as a baseline for feature aggregation (Bricken et al., 2024). However, motivated by the specific demands of financial sequence modeling, we propose an alternative, employing sparse feature summing across tokens. This method provides a magnitude-scaled count of how frequently a feature appears within a sequence, reflecting both the number of tokens a feature is active for and its intensity (Lan et al., 2024).

Our approach is inspired by analogous methodologies in literature. For example, Loughran et al. (2009) highlight the value of summing word counts in financial text analysis to derive domain insights.

We sum sparse features, across tokens, from an SAE (EleutherAI, 2024) applied at the layer occurring 90% of the way through the model. At this layer, we capture relevant features from preceding layers via the skip connection (Vaswani et al., 2017), but not the logic-related features that tend to occur at the very last layers (Ghilardi et al., 2024).

The skip connection ensures that a single SAE captures the entire residual stream (Longon, 2024), inherently including information from all preceding layers, thus ensuring that the summed sparse features represent a comprehensive aggregation of the descriptions’s representation in the model.

We analyze summed sparse features, and observe an interesting exponential decay pattern in feature activation frequencies, where half the features never activate, a fourth activate once, an eighth activate twice, and so forth (Figure 1).

Figure 1 highlights the sparsity of LLM latent features – even when these are summed across thousands of tokens – motivating feature summing as

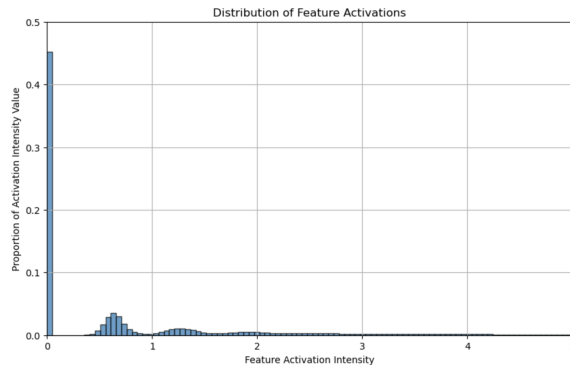


Figure 1: Distribution of summed feature activations for the whole dataset.

an approach. In this context, before summing, a single active feature has, on average, a value of ≈ 0.7 (the first bulge).

This method also addresses a limitation in using embeddings as opposed to sparse features (Vamvourellis et al., 2023), which requires equal-length sequences for comparison. By focusing on cumulative feature occurrences, summed sparse features enable comparisons between sequences of arbitrary lengths, offering greater flexibility for analyzing variable-length financial datasets.

2.3 Models

2.3.1 Embedders

As a baseline, we replicate Vamvourellis et al. (2023)’s embedding methodology and obtain embeddings for company descriptions in our dataset. In particular, we use:

1. BERT: Given the maximum token length of 512, we employ chunking by splitting company descriptions into overlapping chunks of 512 tokens, extracting CLS embeddings for each chunk, and averaging these embeddings to generate a single 1536-token representation, following (Vamvourellis et al., 2023).
2. Sentence-BERT (SBERT): Building on BERT, SBERT improves latency substantially (Reimers and Gurevych, 2019) and encodes meaning on the more abstract sentence level. We again employ chunking to 1536 tokens.
3. PaLM-gecko: Pathways Language Model (PaLM) (Chowdhery et al., 2022).

2.4 Siamese Networks

Given the comparative nature of our use case, we employ Siamese neural networks (Bromley et al.,

1993) to validate the meaningfulness of the extracted features. Specifically, the Siamese network is trained to predict the correlation $p_{i,j}$ between two companies i and j ².

The Siamese network uses similarity information to position correlated companies closer together in the feature space. It employs two identical sub-networks with shared weights and parameters (Koch et al., 2015). Features extracted by the SAE from companies A and B , denoted as f_1 and f_2 , are passed through two dense layers, each followed by a ReLU activation, to produce encoded representations z_1 and z_2 . Cosine similarity of z_1 and z_2 is then used in the MSE loss function for network optimization³. We train a new Siamese network for each year, using data from t (1993–2019) to predict $t + 1$ (1994–2020), iterating year by year.

2.5 Clustering

We benchmark our sparse features against embeddings and SIC/BISC-codes, where each SIC/BISC-code is its own cluster.

Each clustering model G_k represents a grouping methodology, where different models, may share the same clustering algorithm but vary by some distance metric or other parameter, for instance G_{C-TS} for the Siamese-derived ultrametric and G_{C-TM} for the Manhattan metric. Within each G_k , clusters are generated on an annual basis, ensuring independence across years (1996–2020). For each year, G_k contains a set of clusters (e.g., $\{C_1, C_2, C_3\}$ in year 1 and $\{C_X, C_Y, C_Z\}$ in year 2), where each cluster C_i holds a unique subset of companies. Further, given G_R and G_S , the Joint models are defined as $G_{R \cap S} = \bigcup_{i,j} (C_i^R \cap C_j^S)$, where $C_i^R \in G_R$ and $C_j^S \in G_S$. We evaluate each clustering model by computing the mean intra-cluster correlation across its clusters, as defined:

$$\text{MeanCorr}(G_k) = \frac{1}{|G_k|} \sum_{C_i \in G_k} \frac{1}{|C_i|} \sum_{(x,y) \in C_i} \rho(x,y)$$

where $\rho(x,y)$ is the Pearson correlation of logged monthly returns for companies x and y . This metric quantifies stock return coherence within clusters, evaluating each clustering method’s effectiveness.

2.5.1 Clustering Embeddings

Each of the embedders we employ is used to define a group/set-of-clusters (G_{embedder}): (a) G_{BERT} ; (b)

²Monthly returns are used over higher-frequency returns to reduce noise from idiosyncratic events (Huang et al., 2009).

³See Appendix E

G_{SBERT} ; (c) $G_{\text{PaLM-gecko}}$ following Vamvourellis et al. (2023). We first reduce the dimensionality of the embeddings using UMAP (McInnes et al., 2020), then generate clusters through Spectral Clustering. See Appendix A for methodology details.

2.5.2 Clustering Sparse Features

Sparse features lack the locality and smoothness of embeddings (Kiros et al., 2015; Bischeke et al., 2019) to define reliable similarity metrics. Moreover, half of the features never activate (See Figure 1) and hence are unrelated to finance, but are present due to the SAE being trained on a generic dataset (Weber et al., 2024). Thus, we cannot directly cluster the sparse features.

To cluster the sparse features, we adopt the graph-theoretic framework of Bonanno et al. (2004), employing Minimum Spanning Trees (MSTs) to extract hierarchical structures from financial data. A fully connected graph is constructed with edge weights representing a particular distance metric (see metrics 1, 2 below). The MST encodes a subdominant ultrametric, with ultrametric distance defined by the maximum edge weight on the unique path between two nodes⁴. We remove edges above a specified weight level⁵, generating clusters directly from the MST. This eliminates the need for additional clustering steps, ensuring stable and interpretable results consistent with Bonanno et al. (2004).

Metric 1: Siamese-derived Metric: This cluster group is constructed using a siamese-derived ultrametric, and will be called G_{C-TS} . First we obtain predicted correlations from the Siamese (SN) model. Then, following (Bonanno et al., 2004) we use these to define a distance metric between stock pairs, where Δt is the time horizon:

$$d_{i,j}(\Delta t) = \sqrt{2(1 - \rho_{i,j}(\Delta t))}.$$

The distance matrix $\mathbf{D}(\Delta t)$ ⁶ is then used to determine the MST connecting the n stocks.

Metric 2: Manhattan Metric: This group, G_{C-TM} , is based on a second metric, $M_{i,j}$, derived from PCA-transformed sparse features, where

⁴To enforce the ultrametric property, we employ single-linkage hierarchical clustering, which groups nodes by iteratively merging the pair of clusters with the smallest maximum distance between any two points. This process inherently satisfies the ultrametric inequality ($d_{ij} \leq \max(d_{ik}, d_{kj})$) by construction.

⁵See Appendix B on edge-weight cutoff optimisation

⁶With this choice, $d_{i,j}(\Delta t)$ fulfills the three axioms of a metric: (i) $d_{i,j}(\Delta t) = 0$ iff $i = j$; (ii) $d_{i,j}(\Delta t) = d_{j,i}(\Delta t)$; (iii) $d_{i,j}(\Delta t) \leq d_{i,k}(\Delta t) + d_{k,j}(\Delta t)$.

131k-dimensional vectors are reduced to 4,000 dimensions⁷. For each pair of companies i and j , $M_{i,j}$ is computed as:

$$M_{i,j} = \sum_{k=1}^{4000} |\text{PCA}_k(\mathbf{f}_i) - \text{PCA}_k(\mathbf{f}_j)|$$

where $M_{i,j}$ serves as a metric⁸ of dissimilarity (Kotsiantis et al., 2001).

2.6 Pairs Trading

Pairs trading assumes correlated stock returns, with traditional strategies often focusing on relative performance diagnostics such as price ratio spreads (Fallahpour et al., 2016).

The dataset is divided into an in-sample period (Jan 2002–Dec 2013) and an out-of-sample period (Jan 2014–Dec 2020), with clusters G_k (G_{C-T1} , SIC-codes, BISC, and their joined variations). The pairs trading strategy involves the following steps:

1. **Pre-selection:** For each cluster $C_i \in G_k$, stock pairs are filtered if the Pearson correlation of their monthly logged returns exceeds 0.9 during the in-sample period.
2. **Co-integration Testing:** Using historical adjusted close data (Jan 2002–Dec 2013) for the pre-selected pairs while standardized for corporate action, an Engle-Granger co-integration test is conducted with the Augmented Dickey-Fuller (ADF) statistic to determine whether the residual spread is stationary. Pairs with a p-value below 0.05 are considered co-integrated.
3. **Ranking and Selection:** Co-integrated pairs are ranked by their ADF test p-values⁹, with the top 80 pairs retained for out-of-sample evaluation (see Table 1). The effectiveness of co-integration within each cluster group G_k is assessed by evaluating the Sharpe ratio of the entire portfolio. The Sharpe ratio quantifies risk-adjusted returns, measuring excess return per unit of risk. We prioritized this over absolute PnL, as higher Sharpe ratios enable leverage to amplify returns, provided practical

⁷We fit PCA globally across 1996–2020 for consistent eigenvectors.

⁸See Appendix C for the full proof

⁹We choose pairs with lower p-values, as they indicate stronger stationarity of the spread, reflecting a stronger co-integration relationship

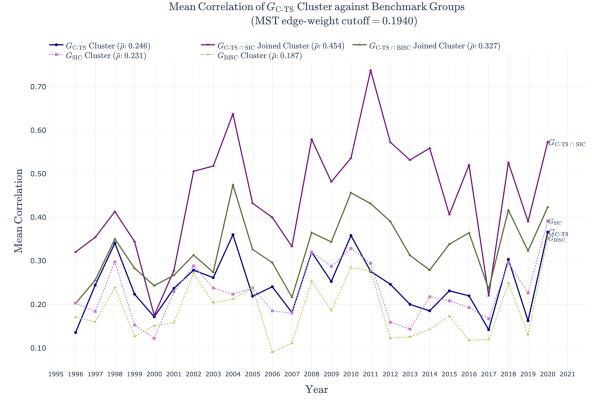


Figure 2: Mean correlation of C-TS (Siamese) Cluster vs Benchmarks between 1996–2020. Joint model significantly outperforming benchmarks, suggesting sparse features and SIC-codes capture complementary, non-overlapping information.

constraints such as transaction costs and risk limits are effectively managed (Guasoni and Mayerhofer, 2018; Peters, 2011).

See Appendix D for Trading Logic Detail.

3 Results

3.1 Clustering Results

For each Sparse-Feature cluster, and their respective joint models¹⁰, we compare (1) MeanCorr(G_k) and (2) Sharpe ratios (See Figure 2, 3). The results demonstrate that pairs derived from our Sparse Features outperform Embeddings, SIC-codes and BISC. Furthermore, the joint models with SIC-codes (i.e. $G_{\text{sparse-feature}} \cap \text{SIC}$) lead to the most granular characterization and the strongest performance in terms of MeanCorr(G_k), more so than the joint embedders cluster groups¹¹. This highlights the complementary nature of traditional and feature-based classification systems (Table 1).

3.2 Pairs Trading Results

During the live trading simulation, cumulative PnL (profits) (Smith and Doe, 2021) and Sharpe ratios (risk-adjusted profits) were recorded for evaluation. Results are reported in Figure 3.

While the co-integration test ensures statistical validity, the strategy’s profitability relies on the underlying structural fundamental similarities between companies. Our clustering approach outperforms SIC & BISC groups in Sharpe ratio, suggest-

¹⁰Joint models are $G_R \cap G_S$ as defined in section 2.5

¹¹Excluding cluster groups marked with *, as they contain missing data that may bias the sample.

Clustering Group (G_k)	MeanCorr(G_k) (1996-2020)	Sharpe Ratio
G_{C-TS}	0.246	12.97
G_{C-TM}	0.266	15.84
G_{BERT}	0.198	12.68
G_{SBERT}	0.219	9.34
$G_{PaLM-gecko}$	0.219	9.97
$G_{C-TS} \cap SIC$	0.454	—
$G_{C-TS} \cap BISC$	0.327	13.88
$G_{C-TM} \cap SIC$	0.416	—
$G_{C-TM} \cap BISC$	0.412	—
$G_{BERT} \cap SIC$	—	12.11
$G_{BERT} \cap BISC$	0.266*	—
$G_{SBERT} \cap SIC$	0.429*	13.49
$G_{SBERT} \cap BISC$	0.292	14.66
$G_{PaLM-gecko} \cap SIC$	0.591*	8.81
$G_{PaLM-gecko} \cap BISC$	0.296	—
SIC	0.231	10.73
BISC	0.187	13.85
Population	0.161	—

Table 1: Performance comparison of clustering algorithms across 1996-2020. For most cluster groups, pairs are formed continuously yearly from 1996–2020. However, years marked with * indicate cluster groups (on a per-year basis) where each cluster had one or no companies, preventing pair formation and introducing potential bias due to data gaps.

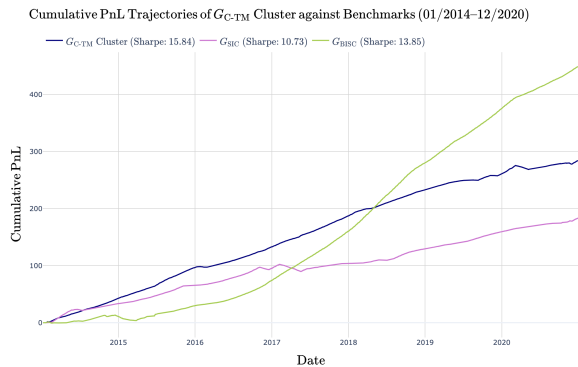


Figure 3: Cumulative PnL and Sharpe ratios comparison between G_{C-TM} Cluster and Benchmarks: G_{C-TM} significantly outperforms in terms of Sharpe

ing our method captures more fundamental aspects of company similarity (Hong and Hwang, 2021).

3.3 Interpretability

Sparse features are understood to be interpretable (Huben et al., 2024), and our core contribution is showing that it is possible to match or improve upon existing methodologies (U.S. Occupational Safety and Health Administration, 2001; Vamvourellis et al., 2023) while imposing an interpretability constraint.

In practice, we use interpretability to ascertain the economic rationale underlying the most co-integrated stock pairs within each cluster C_i in G_{C-TM} . This allows us to go beyond statistical tests on correlation and spread-stationarity, ensuring that the co-integration is supported by valid economic

relationships (Hong and Hwang, 2021).

For each pair of stocks in our portfolio we first obtain an interaction feature vector $f_{i,j}$ by pairwise multiplying the feature vectors s_i, s_j representing the two company descriptions. Then we inspect the features that activate the most across all interaction vectors in our portfolio, and analyze them on the company descriptions of our most co-integrated pair using sae-vis (McDougall, 2024).

The co-integrated pair with the highest Sharpe ratio in G_{C-TM} is **UFP Technologies and Heico**. Both share operational similarities in highly specialized manufacturing: UFP in custom-engineered products for medical and industrial applications; Heico produces aerospace, defense, and industrial components. Many interpretable and relevant features emerge, such as a 'renting' feature 20155 highlighting both companies' niche operations with logistical dependencies, including renting specialized facilities, exposing them to real estate fluctuations. We interpret the feature by examining its impact on the LLM's logic in Appendix F.

3.4 Limitations

The following are the main limitations:

1. We do not fine-tune embedders, LLMs, nor SAEs. This is due to the high computational cost of supervised fine-tuning exceeding our computing budget, though fine-tuning could improve the performance of our method. This is an exciting direction for future work.
2. The exclusion of delisted stocks introduces survivorship bias into the analysis. This can be addressed with more complete data.
3. Our interpretability study is a proof of concept, limited by the availability of human feature annotators (there are tens of thousands of active features), and while we rely on the literature as support for the claim that SAE features are interpretable (Huben et al., 2024), our study could be expanded in the future.

4 Conclusions

We find that using SAE features is an effective and interpretable method for computing company similarity and explaining returns. Stress-testing, portfolio diversification, and other hedging-related strategies could all be subjects of further investigation using our clustering approach. We will release all our datasets and code in the camera ready.

References

- Benjamin Bischke, Patrick Helber, Damian Borth, and Andreas Dengel. 2019. [Multi-task learning for disaster image classification](#). In *2019 IEEE International Geoscience and Remote Sensing Symposium (IGARSS)*, pages 224–227. IEEE.
- G. Bonanno, G. Caldarelli, F. Lillo, S. Micciche, N. Vandewalle, and R. N. Mantegna. 2004. [Networks of equities in financial markets](#). *The European Physical Journal B - Condensed Matter*, 38(2):363–371.
- Trenton Bricken, Jonathan Marcus, Siddharth Mishra-Sharma, Meg Tong, Ethan Perez, Mrinank Sharma, Kelley Rivoire, and Thomas Henighan. 2024. Using dictionary learning features as classifiers. Technical report, Anthropic.
- Trenton Bricken, Adly Templeton, Joshua Batson, Brian Chen, and Adam Jermy. 2023. [Towards monosemanticity: Decomposing language models with dictionary learning](#).
- Jane Bromley, James Bentz, Leon Bottou, Isabelle Guyon, Yann Lecun, Cliff Moore, Eduard Sackinger, and Rookpak Shah. 1993. [Signature verification using a "siamese" time delay neural network](#). *International Journal of Pattern Recognition and Artificial Intelligence*, 7:25.
- Shuangshuang Chen and Wei Guo. 2023. [Autoencoders in deep learning—a review with new perspectives](#). *Mathematics*, 11(8).
- Wanghu Chen, Huijun Li, Jing Li, and Ali Arshad. 2020. [Autoencoder-based outlier detection for sparse, high dimensional data](#). In *2020 IEEE International Conference on Big Data (Big Data)*, pages 2735–2742.
- Aakanksha Chowdhery, Sharan Narang, Jacob Devlin, Maarten Bosma, Gaurav Mishra, Adam Roberts, Paul Barham, Hyung Won Chung, Charles Sutton, Sebastian Gehrmann, Parker Schuh, Kensen Shi, Sasha Tsvyashchenko, Joshua Maynez, Abhishek Rao, Parker Barnes, Yi Tay, Noam Shazeer, Vinodkumar Prabhakaran, Emily Reif, Nan Du, Ben Hutchinson, Reiner Pope, James Bradbury, Jacob Austin, Michael Isard, Guy Gur-Ari, Pengcheng Yin, Toju Duke, Anselm Levskaya, Sanjay Ghemawat, Sunipa Dev, Henryk Michalewski, Xavier Garcia, Vedant Misra, Kevin Robinson, Liam Fedus, Denny Zhou, Daphne Ippolito, David Luan, Hyeontaek Lim, Barret Zoph, Alexander Spiridonov, Ryan Sepassi, David Dohan, Shivani Agrawal, Mark Omernick, Andrew M. Dai, Thanumalayan Sankaranarayanan Pilla, Marie Pellat, Aitor Lewkowycz, Erica Moreira, Rewon Child, Oleksandr Polozov, Katherine Lee, Zongwei Zhou, Xuezhi Wang, Brennan Saeta, Mark Diaz, Orhan Firat, Michele Catasta, Jason Wei, Kathy Meier-Hellstern, Douglas Eck, Jeff Dean, Slav Petrov, and Noah Fiedel. 2022. [Palm: Scaling language modeling with pathways](#). *Preprint*, arXiv:2204.02311.
- Arthur Conmy, Augustine Mavor-Parker, Aengus Lynch, Stefan Heimersheim, and Adrià Garriga-Alonso. 2023. Towards automated circuit discovery for mechanistic interpretability. *Advances in Neural Information Processing Systems*, 36:16318–16352.
- Danile Delphini, Stefano Battiston, Guido Caldarelli, and Massimo Raccaboni. 2019. [Systemic risk from investment similarities](#). *PLOS ONE*.
- Abhimanyu Dubey, Abhinav Jauhri, Abhinav Pandey, Abhishek Kadian, Ahmad Al-Dahle, Aiesha Letman, Akhil Mathur, Alan Schelten, Amy Yang, Angela Fan, Anirudh Goyal, Anthony Hartshorn, Aobo Yang, Archi Mitra, Archie Sravankumar, Artem Korenev, Arthur Hinsvark, Arun Rao, Aston Zhang, Aurelien Rodriguez, Austen Gregerson, Ava Spataru, Baptiste Roziere, Bethany Biron, Binh Tang, Bobbie Chern, Charlotte Caucheteux, Chaya Nayak, Chloe Bi, Chris Marra, Chris McConnell, Christian Keller, Christophe Touret, Chunyang Wu, Corinne Wong, Cristian Canton Ferrer, Cyrus Nikolaidis, Damien Al-lonsius, Daniel Song, Danielle Pintz, Danny Livshits, David Esiobu, Dhruv Choudhary, Dhruv Mahajan, Diego Garcia-Olano, Diego Perino, Dieuwke Hupkes, Egor Lakomkin, Ehab AlBadawy, Elina Lobanova, Emily Dinan, Eric Michael Smith, Filip Radenovic, Frank Zhang, Gabriel Synnaeve, Gabrielle Lee, Georgia Lewis Anderson, Graeme Nail, Gregoire Mialon, Guan Pang, Guillem Cucurell, Hailey Nguyen, Hannah Korevaar, Hu Xu, Hugo Touvron, Iliyan Zarov, Imanol Arrieta Ibarra, Isabel Kloumann, Ishan Misra, Ivan Evtimov, Jade Copet, Jaewon Lee, Jan Geffert, Jana Vranes, Jason Park, Jay Mahadeokar, Jeet Shah, Jelmer van der Linde, Jennifer Billock, Jenny Hong, Jenya Lee, Jeremy Fu, Jianfeng Chi, Jianyu Huang, Jiawen Liu, Jie Wang, Jiecao Yu, Joanna Bitton, Joe Spisak, Jongsoo Park, Joseph Rocca, Joshua Johnstun, Joshua Saxe, Junteng Jia, Kalyan Vasuden Alwala, Kartikeya Upasani, Kate Plawiak, Ke Li, Kenneth Heafield, Kevin Stone, Khalid El-Arini, Krithika Iyer, Kshitiz Malik, Kuenley Chiu, Kunal Bhalla, Lauren Rantala-Yearly, Laurens van der Maaten, Lawrence Chen, Liang Tan, Liz Jenkins, Louis Martin, Lovish Madaan, Lubo Malo, Lukas Blecher, Lukas Landzaat, Luke de Oliveira, Madeline Muzzi, Mahesh Pasupuleti, Mannat Singh, Manohar Paluri, Marcin Kardas, Mathew Oldham, Mathieu Rita, Maya Pavlova, Melanie Kambadur, Mike Lewis, Min Si, Mitesh Kumar Singh, Mona Hassan, Naman Goyal, Narjes Torabi, Nikolay Bashlykov, Nikolay Bogoychev, Niladri Chatterji, Olivier Duchenne, Onur Çelebi, Patrick Alrassy, Pengchuan Zhang, Pengwei Li, Petar Vasic, Peter Weng, Prajjwal Bhargava, Pratik Dubal, Praveen Krishnan, Punit Singh Koura, Puxin Xu, Qing He, Qingxiao Dong, Ragavan Srinivasan, Raj Ganapathy, Ramon Calderer, Ricardo Silveira Cabral, Robert Stojnic, Roberta Raileanu, Rohit Girdhar, Rohit Patel, Romain Sauvestre, Ronnie Polidoro, Roshan Sumbaly, Ross Taylor, Ruan Silva, Rui Hou, Rui Wang, Saghar Hosseini, Sahana Chennabasappa, Sanjay Singh, Sean Bell, Seohyun Sonia Kim, Sergey Edunov, Shaoliang Nie, Sharan Narang, Sharath Rapparthi, Sheng Shen, Shengye Wan, Shruti Bhosale, Shun Zhang, Simon Vandenhende, Soumya Batra, Spencer

Whitman, Sten Sootla, Stephane Collot, Suchin Gururangan, Sydney Borodinsky, Tamar Herman, Tara Fowler, Tarek Sheasha, Thomas Georgiou, Thomas Scialom, Tobias Speckbacher, Todor Mihaylov, Tong Xiao, Ujjwal Karn, Vedanuj Goswami, Vibhor Gupta, Vignesh Ramanathan, Viktor Kerkez, Vincent Gonguet, Virginie Do, Vish Vogeti, Vladan Petrovic, Weiwei Chu, Wenhan Xiong, Wenyan Fu, Whitney Meers, Xavier Martinet, Xiaodong Wang, Xiaoqing Ellen Tan, Xinfeng Xie, Xuchao Jia, Xuewei Wang, Yaelle Goldschlag, Yashesh Gaur, Yasmine Babaei, Yi Wen, Yiwen Song, Yuchen Zhang, Yue Li, Yuning Mao, Zacharie Delpierre Coudert, Zheng Yan, Zhengxing Chen, Zoe Papakipos, Aaditya Singh, Aaron Grattafiori, Abha Jain, Adam Kelsey, Adam Shajnfeld, Adithya Gangidi, Adolfo Victoria, Ahuva Goldstand, Ajay Menon, Ajay Sharma, Alex Boesenberg, Alex Vaughan, Alexei Baeovski, Allie Feinstein, Amanda Kallet, Amit Sangani, Anam Yunus, Andrew Lupu, Andres Alvarado, Andrew Caples, Andrew Gu, Andrew Ho, Andrew Poulton, Andrew Ryan, Ankit Ramchandani, Annie Franco, Aparajita Saraf, Arkabandhu Chowdhury, Ashley Gabriel, Ashwin Bharambe, Assaf Eisenman, Azadeh Yazdan, Beau James, Ben Maurer, Benjamin Leonhardi, Bernie Huang, Beth Loyd, Beto De Paola, Bhargavi Paranjape, Bing Liu, Bo Wu, Boyu Ni, Braden Hancock, Bram Wasti, Brandon Spence, Brani Stojkovic, Brian Gamido, Britt Montalvo, Carl Parker, Carly Burton, Catalina Mejia, Changan Wang, Changkyu Kim, Chao Zhou, Chester Hu, Ching-Hsiang Chu, Chris Cai, Chris Tindal, Christoph Feichtenhofer, Damon Civin, Dana Beaty, Daniel Kreymer, Daniel Li, Danny Wyatt, David Adkins, David Xu, Davide Testuggine, Delia David, Devi Parikh, Diana Liskovich, Didem Foss, Dingkan Wang, Duc Le, Dustin Holland, Edward Dowling, Eissa Jamil, Elaine Montgomery, Eleonora Presani, Emily Hahn, Emily Wood, Erik Brinkman, Esteban Arcaute, Evan Dunbar, Evan Smothers, Fei Sun, Felix Kreuk, Feng Tian, Firat Ozgenel, Francesco Caggioni, Francisco Guzmán, Frank Kanayet, Frank Seide, Gabriela Medina Florez, Gabriella Schwarz, Gada Badeer, Georgia Swee, Gil Halpern, Govind Thattai, Grant Herman, Grigory Sizov, Guangyi, Zhang, Guna Lakshminarayanan, Hamid Shojanazeri, Han Zou, Hannah Wang, Hanwen Zha, Haroun Habeeb, Harrison Rudolph, Helen Suk, Henry Aspegren, Hunter Goldman, Igor Molybog, Igor Tufanov, Irina-Elena Veliche, Itai Gat, Jake Weissman, James Geboski, James Kohli, Japhet Asher, Jean-Baptiste Gaya, Jeff Marcus, Jeff Tang, Jennifer Chan, Jenny Zhen, Jeremy Reizenstein, Jeremy Teboul, Jessica Zhong, Jian Jin, Jingyi Yang, Joe Cummings, Jon Carvill, Jon Shepard, Jonathan McPhie, Jonathan Torres, Josh Ginsburg, Junjie Wang, Kai Wu, Kam Hou U, Karan Saxena, Karthik Prasad, Kartikay Khandelwal, Katayoun Zand, Kathy Matosich, Kaushik Veeraraghavan, Kelly Michelena, Keqian Li, Kun Huang, Kunal Chawla, Kushal Lakhotia, Kyle Huang, Lailin Chen, Lakshya Garg, Lavender A, Leandro Silva, Lee Bell, Lei Zhang, Liangpeng Guo, Licheng Yu, Liron Moshkovich, Luca Wehrstedt, Madian Khabsa, Manav Avalani, Manish Bhatt, Maria Tsim-

poukelli, Martynas Mankus, Matan Hasson, Matthew Lennie, Matthias Reso, Maxim Groshev, Maxim Naumov, Maya Lathi, Meghan Keneally, Michael L. Seltzer, Michal Valko, Michelle Restrepo, Mihir Patel, Mik Vyatskov, Mikayel Samvelyan, Mike Clark, Mike Macey, Mike Wang, Miquel Jubert Hermoso, Mo Metanat, Mohammad Rastegari, Munish Bansal, Nandhini Santhanam, Natascha Parks, Natasha White, Navyata Bawa, Nayan Singhal, Nick Egebo, Nicolas Usunier, Nikolay Pavlovich Laptev, Ning Dong, Ning Zhang, Norman Cheng, Oleg Chernoguz, Olivia Hart, Omkar Salpekar, Ozlem Kalinli, Parkin Kent, Parth Parekh, Paul Saab, Pavan Balaji, Pedro Rittner, Philip Bontrager, Pierre Roux, Piotr Dollar, Polina Zvyagina, Prashant Ratanchandani, Pritish Yuvraj, Qian Liang, Rachad Alao, Rachel Rodriguez, Rafi Ayub, Raghotham Murthy, Raghu Nayani, Rahul Mitra, Raymond Li, Rebekkah Hogan, Robin Battey, Rocky Wang, Rohan Maheswari, Russ Howes, Ruty Rinott, Sai Jayesh Bondu, Samyak Datta, Sara Chugh, Sara Hunt, Sargun Dhillon, Sasha Sidorov, Satadru Pan, Saurabh Verma, Seiji Yamamoto, Sharadh Ramaswamy, Shaun Lindsay, Shaun Lindsay, Sheng Feng, Shenghao Lin, Shengxin Cindy Zha, Shiva Shankar, Shuqiang Zhang, Shuqiang Zhang, Sinong Wang, Sneha Agarwal, Soji Sajuyigbe, Soumith Chintala, Stephanie Max, Stephen Chen, Steve Kehoe, Steve Satterfield, Sudarshan Govindaprasad, Sumit Gupta, Sungmin Cho, Sunny Virk, Suraj Subramanian, Sy Choudhury, Sydney Goldman, Tal Remez, Tamar Glaser, Tamara Best, Thilo Kohler, Thomas Robinson, Tianhe Li, Tianjun Zhang, Tim Matthews, Timothy Chou, Tzook Shaked, Varun Vontimitta, Victoria Ajayi, Victoria Montanez, Vijai Mohan, Vinay Satish Kumar, Vishal Mangla, Vlad Ionescu, Vlad Poenaru, Vlad Tiberiu Mihalescu, Vladimir Ivanov, Wei Li, Wenchen Wang, Wenwen Jiang, Wes Bouaziz, Will Constable, Xiaocheng Tang, Xiaofang Wang, Xiaoqian Wu, Xiaolan Wang, Xide Xia, Xilun Wu, Xinbo Gao, Yanjun Chen, Ye Hu, Ye Jia, Ye Qi, Yenda Li, Yilin Zhang, Ying Zhang, Yossi Adi, Youngjin Nam, Yu, Wang, Yuchen Hao, Yundi Qian, Yuzi He, Zach Rait, Zachary DeVito, Zef Rosnbrick, Zhaoduo Wen, Zhenyu Yang, and Zhiwei Zhao. 2024. *The llama 3 herd of models*. Preprint, arXiv:2407.21783.

Douglas S. Ehrman. 2012. *The Handbook of Pairs Trading*. Wiley Trading.

EleutherAI. 2024. Sae-llama-3-8b-32x. Hugging Face. Model card: "This is a set of sparse autoencoders (SAEs) trained on the residual stream of Llama 3 8B using the RedPajama corpus. The SAEs are organized by layer, and can be loaded using the EleutherAI sae library." Retrieved from <https://huggingface.co/EleutherAI/sae-llama-3-8b-32x>.

Nelson Elhage, Tristan Hume, Catherine Olsson, Nicholas Schiefer, Tom Henighan, Shauna Kravec, Zac Hatfield-Dodds, Robert Lasenby, Dawn Drain, Carol Chen, Roger Grosse, Sam McCandlish, Jared Kaplan, Dario Amodei, Martin Wattenberg, and

- Christopher Olah. 2022. [Toy models of superposition](#). *Preprint*, arXiv:2209.10652.
- Saeid Fallahpour, Hasan Hakimian, Khalil Taheri, and Ehsan Ramezani. 2016. [Pairs trading strategy optimization using the reinforcement learning method: a cointegration approach](#). *Soft Computing*, 20(12):5051–5066. Intraday US stocks' price data is obtained from the FactSet Research Systems, Inc. (FactSet) The sample period is from June 2015 to January 2016.
- Leo Gao, Tom Dupré la Tour, Henk Tillman, Gabriel Goh, Rajan Troll, Alec Radford, Ilya Sutskever, Jan Leike, and Jeffrey Wu. 2024. [Scaling and evaluating sparse autoencoders](#). *Preprint*, arXiv:2406.04093.
- Davide Ghilardi, Federico Belotti, Marco Molinari, and Jaehyuk Lim. 2024. [Accelerating sparse autoencoder training via layer-wise transfer learning in large language models](#). In *Proceedings of the 7th BlackboxNLP Workshop: Analyzing and Interpreting Neural Networks for NLP*, pages 530–550, Miami, Florida, US. Association for Computational Linguistics.
- Paolo Guasoni and Eberhard Mayerhofer. 2018. [The limits of leverage](#). *Mathematical Finance*, 29(1):249–284.
- Sungju Hong and Soosung Hwang. 2021. [In search of pairs using firm fundamentals: Is pairs trading profitable?](#) *SSRN Electronic Journal*.
- Wei Huang, Qianqiu Liu, S. Ghon Rhee, and Liang Zhang. 2009. [Return reversals, idiosyncratic risk, and expected returns](#). *The Review of Financial Studies*, 23(1):147–168.
- Robert Huben, Hoagy Cunningham, Logan Riggs Smith, Aidan Ewart, and Lee Sharkey. 2024. [Sparse autoencoders find highly interpretable features in language models](#). In *The Twelfth International Conference on Learning Representations*.
- Dean Katselas, Baljit K. Sidhu, and Chuan Yu. 2017. [Know your industry: the implications of using static gics classifications in financial research](#). *Accounting and Finance*.
- Ryan Kiros, Yukun Zhu, Ruslan Salakhutdinov, Richard S. Zemel, Antonio Torralba, Raquel Urtasun, and Sanja Fidler. 2015. [Skip-thought vectors](#). In *Proceedings of the 53rd Annual Meeting of the Association for Computational Linguistics and the 7th International Joint Conference on Natural Language Processing (Volume 1: Long Papers)*, pages 329–339.
- Gregory Koch, Richard Zemel, and Ruslan Salakhutdinov. 2015. Siamese neural networks for one-shot image recognition. *Proceedings of the 32nd International Conference on Machine Learning (ICML)*. Department of Computer Science, University of Toronto, Ontario, Canada.
- S. Kotsiantis, D. Kanellopoulos, and P. Pintelas. 2001. [Handling imbalanced datasets: A review](#). In Nada Lavrač, Dragan Gamberger, Ljupčo Todorovski, and Hendrik Blockeel, editors, *Machine Learning and Data Mining in Pattern Recognition*, volume 4453 of *Lecture Notes in Computer Science*, pages 1–12. Springer.
- Michael Lan, Philip Torr, Austin Meek, Ashkan Khakzar, David Krueger, and Fazl Barez. 2024. [Sparse autoencoders reveal universal feature spaces across large language models](#). *arXiv preprint*, 2410.06981v1. Work done during the ERA-Krueger AI Safety Lab internship.
- André Longon. 2024. [Interpreting the residual stream of resnet18](#). *arXiv preprint arXiv:2407.05340*.
- Mico Loretan and William B. English. 2000. [Evaluating changes in correlations during periods of high market volatility](#). *BIS Quarterly Review*.
- Tim Loughran, Bill McDonald, and Hayong Yun. 2009. [A wolf in sheep's clothing: The use of ethics-related terms in 10-k reports](#). *Journal of Business Ethics*, 89(S1):39–49.
- Samuel Marks, Can Rager, Eric J Michaud, Yonatan Belinkov, David Bau, and Aaron Mueller. 2024. [Sparse feature circuits: Discovering and editing interpretable causal graphs in language models](#). *arXiv preprint arXiv:2403.19647*.
- Callum McDougall. 2024. [SAE Visualizer](#). https://github.com/callummcdougall/sae_vis.
- Leland McInnes, John Healy, and James Melville. 2020. [Umap: Uniform manifold approximation and projection for dimension reduction](#). *Preprint*, arXiv:1802.03426.
- George J. Miao. 2014. [High frequency and dynamic pairs trading based on statistical arbitrage using a two-stage correlation and cointegration approach](#). *International Journal of Economics and Finance*, 6(3).
- MSCI. 2020. [Gics methodology 2020](#).
- Neel Nanda, Lawrence Chan, Tom Lieberum, Jess Smith, and Jacob Steinhardt. 2023. [Progress measures for grokking via mechanistic interpretability](#). In *The Eleventh International Conference on Learning Representations*.
- Robert E. Pardo. 1992. Design, testing, and optimization of trading systems. *J. Wiley*.
- Kiho Park, Yo Joong Choe, and Victor Veitch. 2024. [The linear representation hypothesis and the geometry of large language models](#). *Preprint*, arXiv:2311.03658.
- Ole Peters. 2011. [Optimal leverage from non-ergodicity](#). *Quantitative Finance*, 11(11):1593–1602.

- Manda Raghava and Santosh Bharadwaj. 2014. Pairs trading using cointegration in pairs of stocks. Master of finance research project, Saint Mary’s University, Halifax, Nova Scotia, September. Submitted for MFIN 6692 under the direction of Dr. J. Colin Dodds and approved by Dr. Francis Boabang, MFIN Director.
- Nils Reimers and Iryna Gurevych. 2019. [Sentence-bert: Sentence embeddings using siamese bert-networks](#). *CoRR*, abs/1908.10084.
- John Smith and Jane Doe. 2021. [Profit and loss analysis in algorithmic trading strategies](#). *Journal of Financial Analysis*, 15(3):123–145.
- Adly Templeton, Tom Conerly, Jonathan Marcus, Jack Lindsey, Trenton Bricken, Brian Chen, Adam Pearce, Craig Citro, Emmanuel Ameisen, Andy Jones, Hoagy Cunningham, Nicholas L Turner, Callum McDougall, Monte MacDiarmid, C. Daniel Freeman, Theodore R. Sumers, Edward Rees, Joshua Batson, Adam Jermyn, Shan Carter, Chris Olah, and Tom Henighan. 2024. [Scaling monosemanticity: Extracting interpretable features from claude 3 sonnet](#). *Transformer Circuits Thread*.
- U.S. Occupational Safety and Health Administration. 2001. [Standard industrial classification \(sic\) manual](#). Accessed: 2024-11-08.
- U.S. Securities and Exchange Commission. 2023. [Form 10-k: Annual report pursuant to section 13 or 15\(d\) of the securities exchange act of 1934](#). Accessed: 2024-12-02.
- Dimitrios Vamvourellis, Michael Toth, Shubham Bhat, Dhairya Desai, Dhruv Mehta, and Sara Pasquali. 2023. [Company similarity using large language models](#). *arXiv preprint arXiv:2308.08031*. [Online; accessed 2-Dec-2024].
- Ashish Vaswani, Noam Shazeer, Niki Parmar, Jakob Uszkoreit, Llion Jones, Aidan N. Gomez, Łukasz Kaiser, and Illia Polosukhin. 2017. [Attention is all you need](#). In *Proceedings of the 31st International Conference on Neural Information Processing Systems (NeurIPS)*. Curran Associates, Inc.
- Maurice Weber, Daniel Fu, Quentin Anthony, Yonatan Oren, Shane Adams, Anton Alexandrov, Xiaozhong Lyu, Huu Nguyen, Xiaozhe Yao, Virginia Adams, Ben Athiwaratkun, Rahul Chalamala, Kezhen Chen, Max Ryabinin, Tri Dao, Percy Liang, Christopher Ré, Irina Rish, and Ce Zhang. 2024. [Redpajama: an open dataset for training large language models](#). *arXiv preprint arXiv:2411.12372*.
- Winton. 2018. Systematic methods for classifying equities. Technical report, Winton Capital Management Limited (“WCM”).
- Yahoo Finance. 2024. [Yahoo finance](#).

A Clustering Embeddings

For BERT, we used `bert-base-uncased` from the `transformers` library. For SBERT, we used `all-MiniLM-L6-v2` from the `sentence_transformers` library. For PaLM-gecko, we used `textembedding-gecko@003` from the `vertexai` library.

Chunking: In our methodology, for both BERT and SBERT, we followed [Vamvourellis et al. \(2023\)](#) and implemented a chunking mechanism to accommodate the models’ maximum token limit of 512. Specifically, company descriptions exceeding this limit were split into overlapping chunks of 512 tokens. The [CLS] embeddings of these chunks were averaged to generate a single document embedding of 1536 tokens. For PaLM-Gecko, we leveraged its extended context window of 3072 tokens and directly processed the descriptions without chunking.

The pipeline below is optimised through Optuna’s Tree-structured Parzen Estimator (TPE) sampler for Bayesian hyperparameter optimization. The objective function maximizes $\text{MeanCorr}(G_k)$. This search is constrained to 150 trials and a maximum timeout of 9 hours to balance thoroughness and resource usage:

(a) Dimensionality Reduction with UMAP: Given the high dimensionality of the input embeddings (768-dimensional vectors derived from a BERT model), we employ Uniform Manifold Approximation and Projection (UMAP) (?) to reduce these high-dimensional textual embeddings to a lower-dimensional space, preserving both local and global data structures. We optimize three UMAP parameters to improve the quality of the downstream clustering: (1) `n_components` (target dimensionality); (2) `n_neighbors`; and (3) `min_dist`. All embeddings are standardized and casted to `float32` to ensure computational efficiency.

(b) Clustering with Spectral Clustering: After reducing dimensionality, we perform clustering using Spectral Clustering, which is capable of handling noise and complex cluster shapes, following [Vamvourellis et al. \(2023\)](#). We first construct an affinity matrix from a `k`-nearest neighbors (KNN) graph of the UMAP outputs. Spectral Clustering then operates on this graph’s eigenstructure to form clusters. The number of clusters (`n_clusters`) is tuned via Optuna, while the neighborhood size (`k`) is set to a constant of 5, following [Vamvourellis](#)

et al. (2023).

(c) Temporal Cross-Validation: To evaluate the stability and temporal generalization of the resulting clusters, we employ temporal cross-validation. The dataset is split into chronological folds. This setup reduces temporal bias and assesses whether the identified cluster structure remains consistent over time. We used parallel processing to evaluate each fold.

Embedder Cluster Group (G_{embedder})	UMAP $n_{\text{components}}$	UMAP $n_{\text{neighbors}}$	UMAP min_dist
G_{BERT}	7	119	0.109
G_{SBERT}	7	79	0.012
$G_{\text{PaLM-gecko}}$	6	40	0.120

Table 2: Optimized UMAP Thresholds for Embedders

Embedder Cluster Group (G_{embedder})	Spectral n_{clusters}	Spectral $n_{\text{neighbors}}$
G_{BERT}	10	5
G_{SBERT}	49	5
$G_{\text{PaLM-gecko}}$	27	5

Table 3: Optimized Spectral Clustering Thresholds for Embedders

B Clustering Sparse Features

We optimize the cutoffs using Optuna in cross validation. We observe that nearby nodes in the Minimum Spanning Tree (MST) are close in value, indicating a smooth distribution of distances. This is evident in the plot of the edge-weight cutoff threshold (x-axis) against $\text{MeanCorr}(G_k)$ of the resulting cluster groups (y-axis), which shows a continuous and stable trend. The smoothness of the distribution suggests that the underlying sparse features are meaningfully grouped, and the cutoff thresholds effectively preserve local structure while removing noise. This property supports the reliability of the generated clusters and aligns with the ultrametric framework, ensuring interpretability and robustness.

Sparse Feature Cluster Group ($G_{\text{sparse_feature}}$)	MST edge-weight cutoff
$G_{\text{C-TS}}$	0.1940
$G_{\text{C-TM}}$	0.2315

Table 4: Optimized MST edge-weight cutoff Thresholds for Sparse Feature Cluster Group

C Proof of Manhattan metric

To show that $M_{i,j}$ satisfies positive definiteness, we verify the following:

1. **Non-negativity:** By definition,

$$M_{i,j} = \sum_{k=1}^{4000} |\text{PCA}_k(f_i) - \text{PCA}_k(f_j)| \geq 0,$$

as absolute differences are always non-negative.

Zero only for identical points: If $M_{i,j} = 0$, then each term in the sum must be zero, i.e.,

$$\text{PCA}_k(f_i) = \text{PCA}_k(f_j) \quad \forall k.$$

Since the PCA transformation is invertible for features in its span, this implies $f_i = f_j$. Conversely, if $f_i = f_j$, then all differences are zero, so $M_{i,j} = 0$.

2. **Symmetry:** Using the property of absolute values,

$$|\text{PCA}_k(f_i) - \text{PCA}_k(f_j)| = |\text{PCA}_k(f_j) - \text{PCA}_k(f_i)| \quad \forall k.$$

Therefore,

$$M_{i,j} = M_{j,i}.$$

3. **Triangle Inequality:**

For each dimension k , for all l , the absolute value satisfies the triangle inequality:

$$|\text{PCA}_k(f_i) - \text{PCA}_k(f_j)| \leq |\text{PCA}_k(f_i) - \text{PCA}_k(f_l)| + |\text{PCA}_k(f_l) - \text{PCA}_k(f_j)|.$$

Summing over all dimensions k gives:

$$\sum_{k=1}^{4000} |\text{PCA}_k(f_i) - \text{PCA}_k(f_j)| \leq \sum_{k=1}^{4000} |\text{PCA}_k(f_i) - \text{PCA}_k(f_l)| + \sum_{k=1}^{4000} |\text{PCA}_k(f_l) - \text{PCA}_k(f_j)|.$$

This simplifies to:

$$M_{i,j} \leq M_{i,l} + M_{l,j}.$$

Thus, $M_{i,j}$ satisfies the triangle inequality.

D Trading details

In the out-of-sample evaluation (Jan 2014–Dec 2020), we simulated live trading of co-integrated pairs using a mean-reversion strategy.

Following Miao (2014), we assumed zero transaction costs, opening positions when the residual spread deviated beyond $\pm 1\sigma$ its mean, and closing when the spread reverted to the mean. A stop-loss mechanism is triggered if the spread exceeds $\pm 2\sigma$.

We allocated a fixed capital per pair and normalized the daily Total Portfolio Value (cash + unrealized PnL) to enable fair comparisons across clustering methods, regardless of the number of pairs. This normalization ensures that clusters with varying pair counts (e.g., 5 pairs vs. 60 pairs) have comparable portfolio value trajectories, where each pair is traded with an equivalent unit of capital (i.e., \$1). The daily normalized portfolio value series was subsequently used for Sharpe ratio calculations.

E Siamese Hyperparameters

Siamese Network was trained for 10 epochs with a learning rate of 0.001. The loss function used is Mean Squared Error (MSE). The hidden dimensions are 128 and 64 with a ReLU activation function.

F Interpretability of Feature 20155

Token	Logit Contribution
tenant	0.28
tenants	0.24
Tenant	0.23
space	0.23
tenant	0.21
rents	0.21
shell	0.21
office	0.21

Table 5: Logit contribution on the top 8 tokens.